Structure and Dynamics of a Colloidal Silica–Poly(methyl methacrylate) Composite by ^{13}C and ^{29}Si MAS NMR Spectroscopy

Roychen Joseph, Shanmin Zhang, and Warren T. Ford*

Department of Chemistry, Oklahoma State University, Stillwater, Oklahoma 74078

Received July 31, 1995; Revised Manuscript Received October 25, 1995[⊗]

ABSTRACT: A silica–poly(methyl methacrylate) (PMMA) composite was prepared by condensation polymerization of a 2 nm shell of the silane coupling agent 3-(trimethoxysilyl)propyl methacrylate (TPM) on the surface of 10.5 nm diameter sol–gel colloidal silica particles followed by free-radical polymerization of a 50 wt % dispersion of the TPM–silica in methyl methacrylate. Cross-polarization combined with magic angle spinning and high-power decoupling (CP/MAS) and single-pulse ^{29}Si NMR spectra together with quasi-adiabatic cross-polarization (QACP) ^{13}C NMR spectra provided quantitative analyses of the structural components of the parent silica, the TPM–silica, and the composite. The parent silica contained one ethoxy group and eleven hydroxy groups per ten silicon atoms. The TPM–silica contained one residual methoxy group per TPM group and no residual hydroxy groups. Polymerization with MMA consumed 85% of the methacrylate groups of the TPM. Time constants $T_{1\rho H}$ for proton spin–lattice relaxation in the rotating frame detected via ^{13}C and ^{29}Si CPMAS spectra showed rapid spin diffusion between all CH protons in the samples, but not between the CH protons and the OH protons that cross-polarize ^{29}Si atoms in the parent silica. Time constants $T_{1\rho C}$ for carbon spin–lattice relaxation in the rotating frame showed that the TPM–silica has substantial motion at kilohertz frequencies leading to fast relaxation, whereas the PMMA composite is more rigid and the ethoxy groups in the parent silica are more mobile. Measurements of ^1H–^1H dipolar transverse relaxation times via ^{13}C and ^{29}Si detection showed decreasing strengths of homonuclear dipolar interactions due to increasing molecular motion in the order composite > TPM–silica > OH groups in parent silica.

Introduction

Silica–polymer composites are widely employed as structural materials for their high strength and low density, and a new generation of silica composites prepared by sol–gel methods shows promise also as optical materials. The mechanical performance of a composite depends on adhesion at the interface between the dispersed and continuous phases.[1,2] If the surface of the filler, such as glass fibers or colloidal silica, is incompatible with the polymer, the phases separate by agglomeration of the filler. The silica surface can be modified with alkyltrialkoxysilanes, $X(CH_2)_nSi(OR)_3$, known as silane coupling agents, to improve adhesion between the filler and the polymer. The alkoxy groups of the coupling agent hydrolyze to OH groups that condense with the silica surface, and the functionalized alkyl chain is more compatible than the bare surface of the silica with the polymer. The functional group X of the silane coupling agent may be an amine, alcohol, epoxide, or acrylate group that forms covalent bonds with the polymer, or it may just provide an organic coating on the silica that solvates the polymer. The structures of the interfacial regions of composites have been studied by FTIR and NMR spectroscopy, and NMR also has been applied to probe the dynamics of the interface. Understanding of the structures and dynamics of polymer–silica interfaces should aid in the design of materials with improved mechanical and optical properties.

Much smaller domains of silica, and therefore greater interfacial area, are achieved by sol–gel methods of formation of the silica phase of a composite.[3–12] Under neutral or acid-catalyzed conditions, hydrolysis of tetramethyl or tetraethyl orthosilicate in a polymer matrix creates silica domains so small that the composites are optically clear.[12] Small silica domains formed within amorphous organic polymers enhance the mechanical strength and raise the glass transition temperature.[9] In these composites the adhesion between the phases depends on hydrogen bonding or dipolar attraction between the polymer and the silica surface.

The structures of high surface area silica gel, silane coupling agents bound to silica gel, and a few silica–polymer composites have been investigated by cross-polarization combined with magic angle spinning and high-power decoupling (CP/MAS).[13–28] ^{29}Si NMR experiments detect three types of silicon atoms at about −90, −100, and −110 ppm, designated Q^2, Q^3, and Q^4 according to the number of OSi groups bound, as shown below, where R is H or alkyl.

$$Q^2 = (RO)_2Si(OSi)_2$$

$$Q^3 = ROSi(OSi)_3$$

$$Q^4 = Si(OSi)_4$$

Silica gel and sol–gel silica prepared under acidic conditions contain only OH groups, but sol–gel syntheses under basic conditions leave alkoxy groups, such as OCH_2CH_3 from incomplete hydrolysis of tetraethyl orthosilicate (TEOS).[1,4] The relative numbers of Q^2, Q^3, and Q^4 groups in a silica sample depend on its thermal history and on the conditions of drying before analysis. ^1H combined rotation and multiple pulse (CRAMPS) NMR experiments on silica gel detect several kinds of OH protons, which are distinguished by chemical shift and strengths of dipolar interactions: isolated OH groups, hydrogen-bonded OH groups, and physisorbed water.[25] Reactions of surface OH groups with silane

* Phone 405-744-5946, fax 405-744-6007, e-mail wtford@osuunx.ucc.okstate.edu.

[⊗] Abstract published in *Advance ACS Abstracts,* January 1, 1996.

0024-9297/96/2229-1305$12.00/0

coupling agents during the formation of composites or with alkyltrialkoxysilanes during the modification of silica surfaces for chromatography convert Q^2 silicon sites to Q^3 and Q^3 to Q^4, and incorporate a new group of silicon atoms, having ^{29}Si NMR signals at about −48, −57, and −65 ppm, designated T^1, T^2, and T^3, as shown below, where R′ is an alkyl or $(CH_2)_nX$ group.

$$T^1 = (RO)_2Si(OSi)R'$$

$$T^2 = ROSi(OSi)_2R'$$

$$T^3 = Si(OSi)_3R'$$

^{13}C spin−lattice relaxation times and ^2H line shapes in spectra of surface-modified silicas have shown that motion of the alkyl groups is restricted by bonding to the silica surface and that mobilities of the alkyl chains increase with distance from the surface.[29−36] Spectra of silica modified with deuterated (aminopropyl)triethoxysilane (APS) were simulated by superposition of a rigid and a mobile species, with the relative amounts of the species depending on degree of surface coverage.[29−31]

In contrast to high surface area silica gels, the volume fraction of interfacial material is small in composites of silica fiber or beads, and the NMR signals of the interface in such composites can be studied only by isotopic labeling or by use of ultrafine particles. Both approaches have been used to study how the incorporation into a composite of silica modified with a coupling agent affects its motional behavior. Relaxation rates of ^{13}C, and of ^1H detected via ^{13}C, and cross-polarization rates in composites of ^{13}C-labeled APS-modified 5 μm diameter glass beads in nylon-6 were explained by entanglements and interpenetration of the polysiloxane and polyamide networks.[33,34] Overlapping ^{13}C signals prevented measurement of the extent of amide bond formation between the coupling agent and the polyamide. APS-modified amorphous silica in epoxy resins gave $^1H-^{29}Si$ cross-polarization rates indicative of somewhat greater rigidity when the APS was hydrolyzed before incorporation into the epoxy network.[35] $^1H-^{29}Si$ cross-polarization rates also have shown surface interactions between unmodified silica, formed by sol−gel methods, and polymer chains in poly(vinyl alcohol).[36]

We have prepared a new type of silica−polymer composite in which 150 nm diameter colloidal silica particles, formed by hydrolysis of TEOS under basic conditions, are dispersed into monomers such as methyl methacrylate (MMA), and the monomer is polymerized to produce a composite film.[37,38] The monodisperse charged silica can be ordered into a crystal lattice of colloidal particles to produce a composite that is optically clear except at the wavelength where the colloidal crystal Bragg diffracts visible light. To understand the structure and dynamics of the interface between the sol−gel colloidal silica particles and the poly(methyl methacrylate) (PMMA) matrix, we have determined the structures of the materials by CP/MAS NMR spectroscopy and measured relaxation times of the silica particles, the matrix, and the interface created by the silane coupling agent 3-(trimethoxysilyl)propyl methacrylate (TPM). Since the 150 nm silica particles used to prepare the optical materials contained too little TPM to detect the interface well by NMR spectroscopy, we prepared 10.5 nm diameter sol−gel colloidal silica to produce a composite with bulk composition similar to that of the optical materials and a much larger amount of the interface.

Experimental Section

Materials. Tetraethyl orthosilicate (TEOS), 3-(trimethoxysilyl)propyl methacrylate (TPM), and methyl methacrylate (MMA) were distilled under reduced pressure prior to use. Absolute ethanol was freshly distilled. Ammonium hydroxide (30%) and 2,2-dimethoxy-2-phenylacetophenone (DMPA) were used as received.

Analytical Methods. Transmission electron micrographs were obtained with a JEOL JEM-100CX II microscope at 75 kV. One drop of the colloidal dispersion was placed on a sample grid and allowed to stand for 30−40 s, and the solvent was wicked away using filter paper. This procedure was repeated with a 3% uranyl acetate solution to stain the sample. Images of 100 particles were measured on the photographic negative for calculation of the number- and weight-average diameters: D_n = 10.2 nm; D_w = 10.5 nm.

Samples for elemental analysis and for NMR and IR spectrsocopy were ground to a fine powder and dried at 52 °C under vacuum for 24 h. Elemental analyses were performed at Atlantic Microlab Inc.

Colloidal Silica.[39−44] A 5-L round-bottom flask was charged with 75 mL of ammonium hydroxide and 3450 mL of absolute ethanol. With magnetic stirring TEOS (150 mL, 0.2 M) was added rapidly, and the mixture was kept at 22 °C for 10 h. The dispersion contained 1.52 wt % solids (as SiO_2), measured by evaporation of solvent from 0.25−0.50 mL of the dispersion and drying at 120 °C for 3−4 h to constant weight of residue. Anal. C, 2.29 (2.43 mg-atom g^{-1}); H, 1.96 (19.4 mg-atom g^{-1}).

TPM Silica.[40,43] To 2.0 L of silica dispersion (30.4 g of silica) was added 150 mL of TPM, and the mixture was stirred for 2.5 h at 24 °C. The volume of the mixture was reduced to about 750 mL by slow distillation of ethanol at 32 °C under reduced pressure over 7.5 h. Anal. C, 24.30 (20.3 mg-atom g^{-1}); H, 3.70 (36.7 mg-atom g^{-1}).

PMMA−Silica Composite. Regenerated cellulose dialysis tubing (Spectra/Por 7, Spectrum Chemical Co.) was thoroughly washed with distilled water and with absolute ethanol several times. Colloidal dispersion (30 mL) was filled into the tubing and suspended in 300 mL of methanol. The methanol was stirred using a magnetic stirrer and replaced 5−6 times with fresh methanol over a period of 2 days until the ethanol was completely removed according to the proton NMR spectrum of the dispersion. Dialysis also removed the unbound TPM. The dispersion was concentrated by distillation under vacuum to 75 mL (10.6 wt % solids). A similar dialysis procedure was used to transfer the particles from methanol into MMA. The dispersion in MMA was concentrated to 50 wt % solids by slowly bubbling argon gas through the dispersion with stirring.

A 396 μm thick photochemical cell was made using three 132 μm Teflon spacers sandwiched between two 762 × 508 × 1 mm glass slides. Three sides of the cell were sealed with epoxy resin at room temperature (Devcon 5 Minute Epoxy, Devcon Corp.), and the Teflon spacer was removed. About 2 mL of the colloidal dispersion in MMA was added to the photoinitiator (DMPA, 1 wt % of monomer). The solution was purged with nitrogen for 1 min and injected into the photochemical cell. The fourth side of the cell was sealed with epoxy resin and cured at room temperature for 5 min. The cell was placed vertically 7.9 cm from a 450 W medium-pressure mercury lamp in a water-cooled quartz immersion jacket and irradiated 4 h at 39 °C. About 9.65 g of the composite was prepared from six such samples. The cell was cut open to recover the composite.

CP/MAS NMR Spectroscopy. Solid-state ^{13}C NMR spectra at 75.7 MHz were recorded at 18−19 °C on a Chemagnetics CMX-300 NMR spectrometer equipped with solid-state probes using 5 and 7.5 mm MAS zirconia rotors holding 150−200 and 600−700 mg of samples, respectively. All cross-polarization experiments employed the quasi-adiabatic cross-polarization method,[45] which effectively compensates the Hartmann−Hahn mismatch effect. Typical measurement conditions were as follows: ^1H 90° pulse width, 5 μs; cross-polarization (CP) contact time, 2 ms; spinning frequency, 4 kHz; decoupling and

Scheme 1

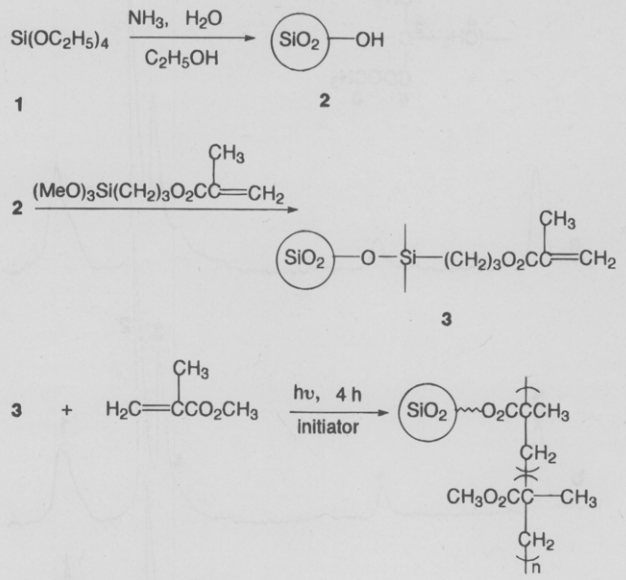

CP pulse strengths, 50 kHz; spectral width, 50 kHz. Chemical shifts were referred to the aromatic carbon peak of hexamethylbenzene (132.2 ppm). ^{29}Si NMR were obtained at 59.8 MHz with 2 kHz MAS and a proton 90° pulse width of 6 μs, corresponding to cross-polarization and decoupling pulse strengths of 42 kHz and a CP contact time of 5 ms. The chemical shift was referenced using the sodium salt of 2-(trimethylsilyl)ethanesulfonic acid (1.7 ppm from TMS). Single-pulse experiments were done with a ^{29}Si 90° pulse width of 5 μs and a 200 s delay between acquisitions for relaxation to obtain quantitative spectra.

Results

Syntheses. The synthetic scheme for the composite is shown in Scheme 1. Colloidal silica (**2**) was synthesized by hydrolysis of tetraethyl orthosilicate (TEOS, **1**) with ammonia and water in ethanol by the Stöber method[39–44] using conditions empirically determined by Bogush and Zukoski[44] to produce 11–12 nm diameter particles. The average particle diameter of our sample was 20 nm by dynamic light scattering, and transmission electron microscopy showed aggregated primary particles of 10.5 nm weight-average diameter (Figure 1). By elemental analysis the parent silica particles contained substantial amounts of carbon and hydrogen, as reported before.[41–43] The compositions calculated from the analyses, reported in Table 1, correspond to one ethoxy group and eleven OH groups, from SiOH and water, per ten Si atoms.

TPM was polymerized onto the surface of the parent silica particles to form TPM–silica (**3**). The ^{29}Si NMR and IR spectra showed that the surface of the parent silica was altered, and TEM showed both greater aggregation of particles and poorer resolution than the TEM of the parent silica in Figure 1. The amount of TPM incorporated corresponds with an average TPM shell thickness of 2 nm on 10.5 nm diameter parent silica spheres, based on increased carbon content from elemental analysis (Table 1), a density of the parent silica of 2.05 g cm^{-3},[41] an estimated density of the TPM shell of 1.12 g cm^{-3}, and the relative areas of ^{29}Si peaks in the single-pulse NMR spectrum. Elemental analysis of the TPM–silica combined with silicon composition from ^{29}Si peak areas gave the calculated compositions in Table 1. The data indicate that the TPM–silica retained the OC_2H_5 groups and lost all of the SiOH groups from the parent colloidal silica. Loss of the OH groups from the parent silica proves that TPM grafted

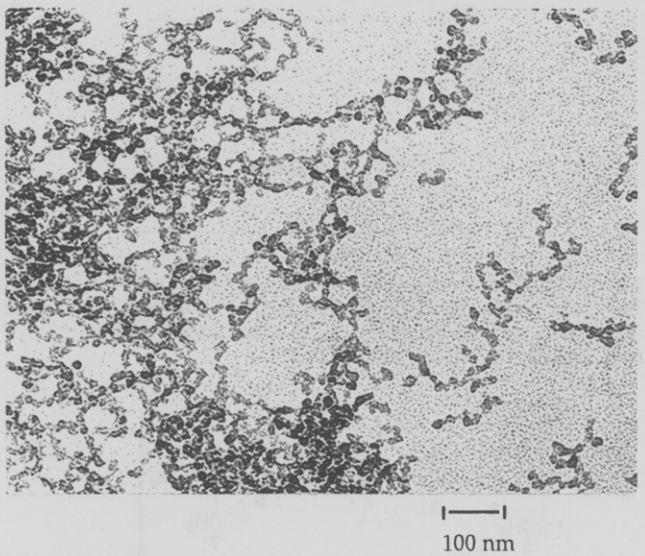

Figure 1. Transmission electron micrograph of parent silica particles.

Table 1. Compositions from Elemental Analyses

group, mmol g−1	parent silica	TPM–silica
OC_2H_5	1.22	0.85
OH	13.3	0.0
TPM		2.3

to the surface, but we cannot rule out the possibility of concurrent formation of new poly-TPM particles too small to detect with our transmission electron microscope.

The volume of ethanol, water, and ammonia in the dispersion was reduced by distillation under vacuum, and the remaining ethanol and water were replaced with methanol by dialysis. Similarly, the methanol was replaced with methyl methacrylate (MMA) by dialysis, and the volume was reduced further by distillation under vacuum to reach a dispersion of about 50.35 wt % TPM–silica particles in MMA. The MMA dispersion was photopolymerized in thin glass cells to produce the composite. On a weight basis the composite contains about 25% parent silica, 25% TPM, and 50% PMMA.

NMR Spectral Analyses of the Structures. ^{13}C CP/MAS spectra of the colloidal silica, the TPM–silica, and the silica–PMMA composite were obtained by the quasi-adiabatic cross-polarization method (QACP).[45] This pulse sequence, shown in Figure 2, uses a constant ^{1}H spin-locking pulse and stepwise increases of the X nucleus pulse strength over a range that brackets the usual Hartmann–Hahn matching condition, $\omega_H = \omega_X$. The sequence is insensitive to mismatch conditions and is especially effective for obtaining high signal-to-noise cross-polarization spectra from weakly heteronuclear dipolar-coupled X nuclei and under high-speed MAS conditions.

Incomplete hydrolysis and condensation leave residual ethoxy groups in the colloidal silica sample, which are detected by peaks at 18 and 61 ppm in the ^{13}C CP/MAS spectrum. These signals are retained in the ^{13}C spectrum of the TPM–silica (Figure 3), which has eight additional signals, in agreement with an earlier report of TPM-modified silica gel.[23] Since the peak due to the OCH_3 group at 51 ppm has the same area as the peaks due to the 3-silylpropyl methacrylate group, the TPM–silica contains one methoxy group per residue of TPM.

Figure 4 compares a ^{13}C CP/MAS spectrum of the composite with a spectrum of PMMA taken one right after the other. Small differences in chemical shifts of

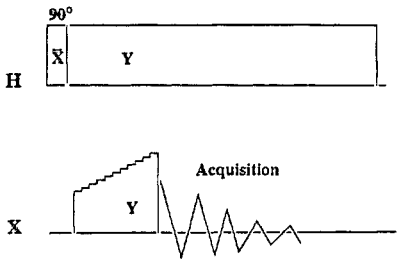

Figure 2. Quasi-adiabatic cross-polarization pulse sequence. The pulse strength of the *X* channel was ramped in 11 equal steps from 39.0 to 61.0 kHz in ^{13}C experiments and from 32.8 to 51.2 kHz in ^{29}Si experiments.

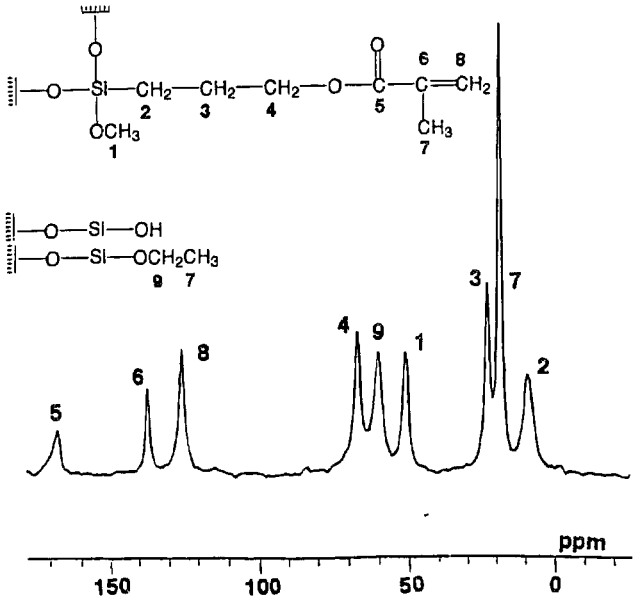

Figure 3. ^{13}C CPMAS NMR spectrum of TPM–silica.

the OCH_3 peaks at 52 ppm and the quaternary C peaks at 45 ppm cause inverted peaks in the difference spectrum. Peaks of components of the composite due to the polymerized TPM appear in the difference spectrum at about 8–10, 20–25, and 60–70 ppm. A small peak at 168 ppm in the spectrum of the composite is due to the carbonyl carbon of unpolymerized methacrylate groups. The ratio of areas of the 168 and 178 ppm peaks is 3/97. Since TPM accounts for 20% of the ester groups in the composite, only 15% (3/20) of the TPM methacrylate groups failed to polymerize. In contrast, a silica gel surface modified with vinyltriethoxysilane retained 67% of its vinyl groups when polymerized with MMA.[46] The major part of the peak at 125 ppm is a spinning sideband of the carbonyl carbon peak at 178 ppm. Small spinning sidebands of the methoxy peak also appear at 106 and 0 ppm.

The QACP pulse sequence was also used to obtain the ^{29}Si cross-polarization spectra. The ^{29}Si spectrum of the parent silica has three signals from Q^2, Q^3, and Q^4 silicon atoms at −90, −100, and −110 ppm,[40] and the spectrum of the TPM–silica (Figure 5a) has a new group of signals at −48 to −65 ppm from ^{29}Si nuclei, designated T^1, T^2, and T^3 silicon atoms, as shown in Figure 5a. The ^{29}Si CPMAS spectrum of the composite has six peaks, similar to the spectrum of the TPM–silica.

More nearly quantitative ^{29}Si NMR spectra were obtained using single-pulse (SP) experiments with a 200 s delay between acquisitions. A preliminary study showed that the average T_1 values for the Q^3 and Q^4 ^{29}Si peaks in the colloidal silica spectrum were about 28 and 40 s, respectively, but that the relaxation at the

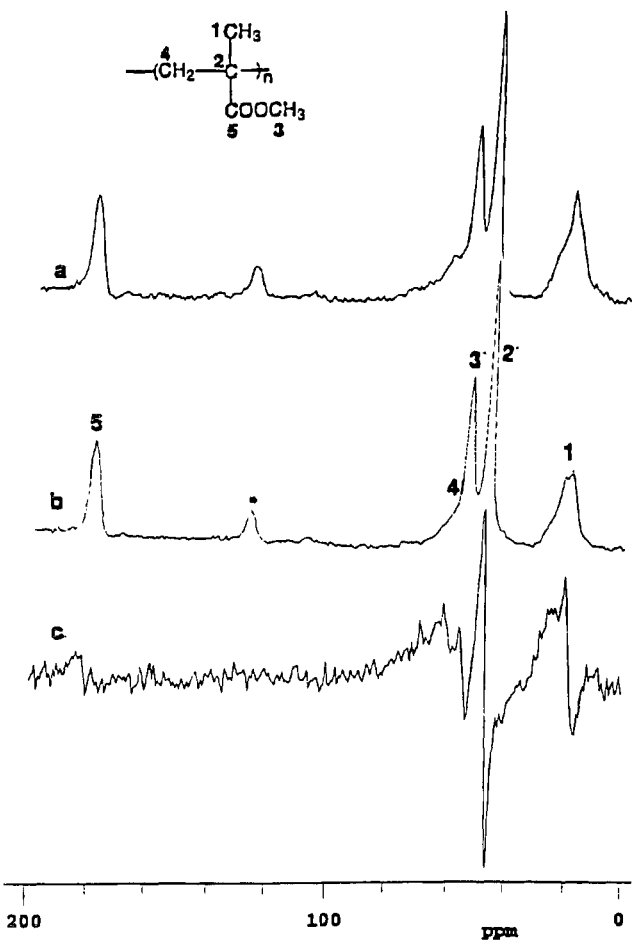

Figure 4. ^{13}C CPMAS NMR spectra of (a) composite and (b) PMMA. Spectrum c is the difference spectrum of (a) − (b).

Q^4 site does not follow a single-exponential function, as shown in Figure 6. This indicates a distribution of relaxation times for Q^4 sites. Deconvoluted ^{29}Si spectra were generated using a function consisting of three overlapping Gaussian lines to obtain a best fit to the experimental spectra, such as that shown in Figure 5b. The quantitative analyses in Table 2 still slightly underestimate the fraction of Q^4 silicon atoms in the materials. The relative peak areas of the T signals and the Q signals of Figure 5b reveal that about 22% of the total Si sites of the TPM–silica are from the coupling agent. The decrease of Q^3 peak area and increase of Q^4 peak area on conversion of the parent silica to TPM–silica (Table 2) shows that Q^3 sites are transformed to Q^4 sites. The molar, weight, and volume percent compositions of all three samples were calculated from the ^{29}Si NMR and elemental analytical data, and the results are reported in Table 3.

The approximately equal areas of the $SiOCH_3$ and the C(2), C(3), and C(4) peaks of the TPM groups in the ^{13}C CP/MAS spectrum of the TPM–silica (Figure 3) indicate one OCH_3 group per methacryloxypropyl group. In addition, the excess of T^3 over T^1 silicon peak area in the quantitative ^{29}Si NMR spectrum (Table 2) indicates an average of less than one (OCH_3 + OH) group per T silicon atom. Although these observations are not in quantitative agreement, together they require that all of the SiOR groups on T^1 and T^2 silicon atoms are from $SiOCH_3$ groups, and none are from SiOH groups.

The percent of Q^4 Si atoms detected in a CP/MAS experiment with a 5-ms contact time was calculated as follows. Assume all Q^4 sites are fully relaxed after an

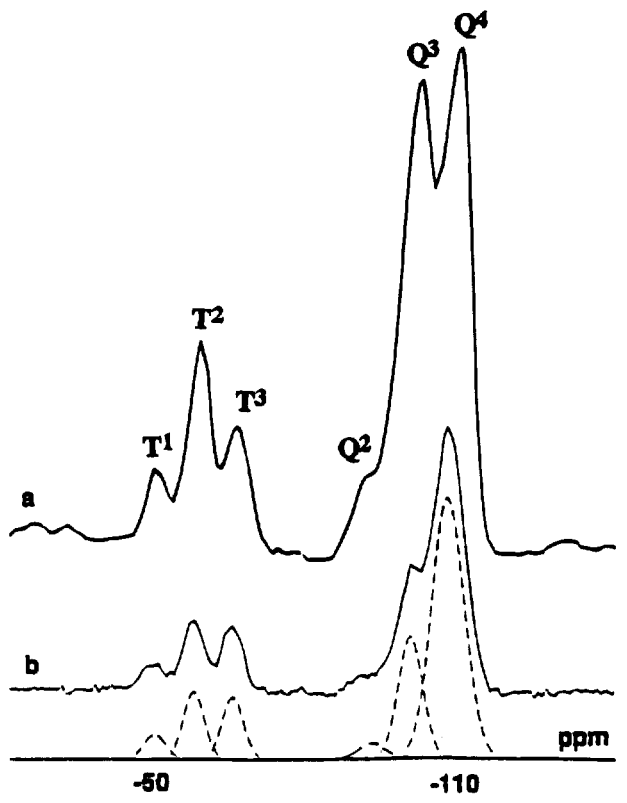

Figure 5. ^{29}Si MAS NMR spectra of TPM–silica: (a) cross-polarization; (b) direct-polarization with 200 s delay between acquisitions. The dashed line is the simulation of spectrum b.

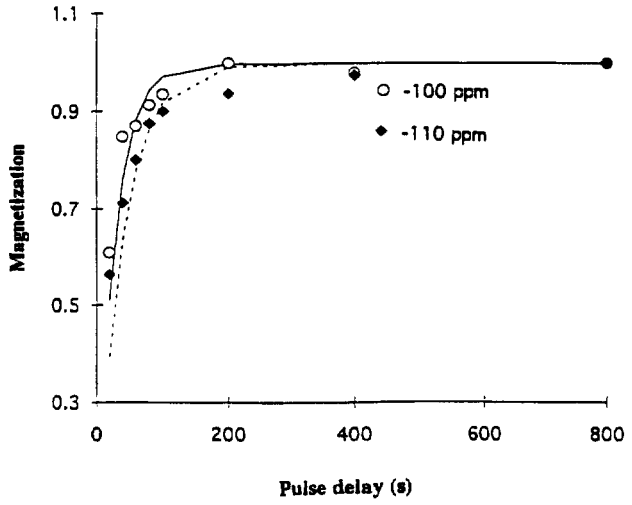

Figure 6. Saturation–recovery ^{29}Si T_1 measurement of parent silica. Open circles are data for the Q^3 Si peak at −100 ppm. Filled squares are data for the Q^4 Si peak at −110 ppm. Curved lines are fits of a single-exponential function to the data.

Table 2. Percentage of Si Atoms from ^{29}Si Direct Polarization Spectra

sample	Q^2	Q^3	Q^4	T^1	T^2	T^3
parent silicaa	3	35	62			
TPM–silica[a]	3	25	72	17	43	40
composite[a]	3	21	76	22[b]	37[b]	41[b]

[a] Estimated errors ± 1. [b] Estimated errors ± 3.

800-s delay in SP spectra as shown in Figure 6. The intensity of the Q^4 signal after a 200-s delay is 93% that of the signal after a 800-s delay, so the relative areas in SP spectra reported in Table 2 account for 93% of the Q^4 Si atoms. Normalization of the parent silica results in Table 2 gives 3% Q^2, 33% Q^3, and 64% Q^4 Si atoms. The relative peak areas in the CP spectrum of the parent silica were 6% Q^2, 66% Q^3, and 28% Q^4. Assuming that both CP and SP spectra detect the Q^2 and Q^3 peaks quantitatively, the percentages of Si atoms detected in the CP spectrum are 3% Q^2, 33% Q^3, and 14% Q^4. Therefore, only (14/64)(100) = 22% of the Q^4 atoms and a total of only 50% of all of the Si atoms in the sample are detected in the CP spectrum. The Q^4 Si atoms not detected in the parent silica sample are not detected in the TPM–silica and composite samples either.

Table 3. Compositions from ^{29}Si NMR Analyses

	mol %			wt %			vol %		
	SiO_2	TPM	PMMA	SiO_2	TPM	PMMA	SiO_2	TPM	PMMA
TPM–silica	78	22		49	51		35	65	
composite	40	11	49	25	25	50	16	29	54

Table 4. $T_{1\rho H}$ (ms) via ^{13}C and ^{29}Si Detection[a]

peak	parent silica	TPM–silica	composite	PMMA
$-C{=}O$ (PMMA)			13	12
$-C{=}O$ (TPM)		3.3		
$-C{=}$		5.5		
$=CH_2$		4.4		
−OCH2		4.7		
$-OCH_2CH_3$	52	5.6		
$-OCH_3$		5.8	13	14
$-C-$			13	14
$-SiCH_2CH_2$		5.6		
$-CCH_3$	42	5.5	12	14
$-SiCH_2$		5.6		
Q^4	31	4.8	9	
Q^3	29	4.8	9	
Q^2	26	5.0		
T^3		4.0	11	
T^2		5.0	11	
T^1			12	

[a] Estimated error limits ±10%.

NMR Relaxation Times. Proton spin–lattice relaxation times, T_{1H}, of all three samples were measured via ^{13}C and ^{29}Si detection. Among the signals of each spectrum, all had the same T_{1H} within experimental error: 0.6 ± 0.1 s for five signals of parent silica, 0.52 ± 0.07 s for fifteen signals of TPM–silica, and 0.53 ± 0.06 s for eight signals of the composite. The T_{1H} values of PMMA measured via ^{13}C detection were the same as those of the composite.

Proton rotating frame spin–lattice relaxation times, $T_{1\rho H}$, of all three samples were measured via ^{13}C and ^{29}Si detection of every peak in the spectra, using a standard pulse sequence, in which the protons are spin-locked for a variable time before cross-polarization, to produce the data in Table 4.

Carbon rotating frame spin–lattice relaxation times $T_{1\rho C}$ were measured by a standard pulse sequence in which the ^{13}C nuclei are cross-polarized, spin-locked for a variable time τ without any ^{1}H power, and detected with ^{1}H decoupling. Since the data sets did not fit a single-exponential function, the $T_{1\rho C}$ values calculated from the first 4 or 5 data points at $\tau \leq 2$ ms are reported in Table 5. We will interpret the $T_{1\rho C}$ data later.

Time constants for proton–proton dipolar dephasing, T_{DH}, were measured via the pulse sequence of Figure 7. This is a ^{1}H spin–echo experiment detected by cross-polarization to ^{13}C and ^{29}Si. The linear semilogarithmic plots of peak height vs delay time τ gave the T_{DH} data in Table 6.

The pulse sequence of Figure 8 was used to measure proton transverse relaxation times, T_{2H}, and to demonstrate spin diffusion from Q^2 sites of parent silica to the

Table 5. $T_{1\rho C}$ (ms)[a]

peak	parent silica	TPM–silica	composite	PMMA
–*C*=O (PMMA)			103	105
–*C*=O (TPM)		55		
–*C*=		30		
=*C*H$_2$		8		
–O*C*H$_2$		7		
–O*C*H$_2$CH$_3$	65	12		
–O*C*H$_3$		27	50	65
–*C*–			130	140
–SiCH$_2$*C*H$_2$		7		
–*C*CH$_3$	80	42	25	20
–Si*C*H$_2$		7		

[a] Estimated error limits ± 10%. All values were calculated from data at τ = 2 ms.

Table 6. Proton Dipolar Dephasing Time Constants (T_{DH}, μs)[a]

peak	parent silica	TPM–silica	composite	PMMA
–*C*=O (PMMA)			7	8
–*C*=O (TPM)		29		
–*C*=		30		
=*C*H$_2$		65		
–O*C*H$_2$		36		
–O*C*H$_2$CH$_3$	24	21		
–O*C*H$_3$		25	8	8
–*C*–			7	8
–SiCH$_2$*C*H$_2$		29		
–*C*CH$_3$	30	33	9	8
–Si*C*H$_2$		25		
Q^4	47	18	12	
Q^3	80	18	13	
Q^2	85			
T^3		25	9	
T^2		20	10	
T^1		21	9	

[a] Estimated error limits ±10%.

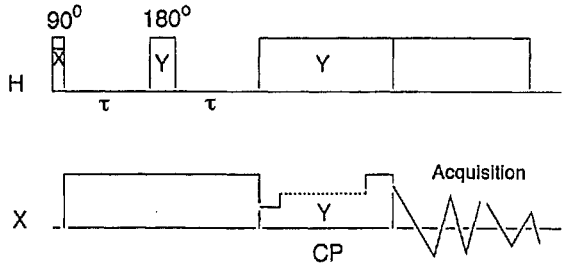

Figure 7. Pulse sequence for measurement of proton–proton dipolar dephasing time constant T_{DH}.

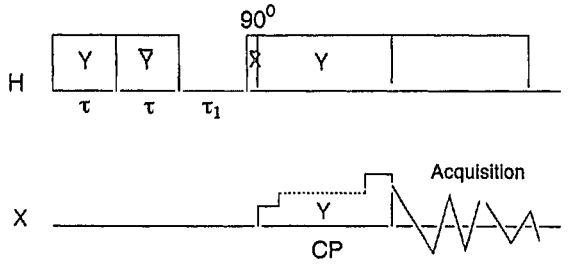

Figure 8. Pulse sequence for measurement of T_{2H} and for qualitative demonstration of spin diffusion.

Q^4 sites. Under strong pulse conditions, the proton magnetization decays under the interaction of a dipolar secular term ($-1/2\mathcal{M}d\gamma$)[47] during 2τ. It is equivalent to a normal T_2 decay after a single 90° pulse, except the chemical shift interaction is removed by the strong pulses, and the remaining magnetization is rotated back to the external magnetic B_0 field to allow spin diffusion. When two ^{1}H pulses of opposite phase are followed by a time period τ_1 of milliseconds for spin diffusion,

Table 7. T_{2H} (μs) via ^{29}Si Detection[a]

peak	parent silica	TPM–silica	composite
Q^4	78	48	35
Q^3	135	46	35
Q^2	148[b]	45	
T^3		72	28
T^2		58	26
T^1		55	25

[a] Estimated error limits ±10%. [b] Estimated error limit ±15%.

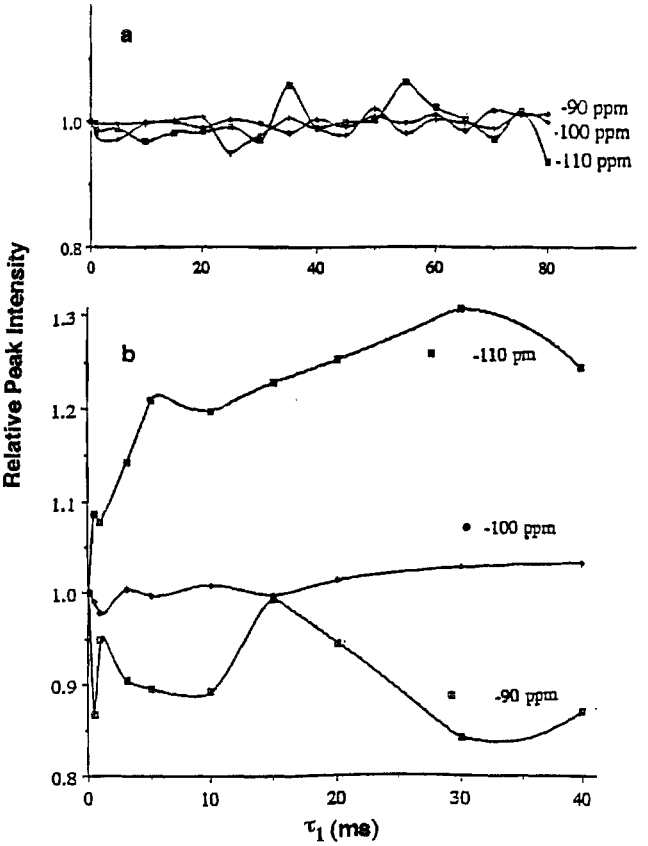

Figure 9. Ratios of intensities of the Q^2, Q^3, and Q^4 ^{29}Si peaks after delay τ_1 to intensities after τ_1 = 0 obtained by the pulse sequence of Figure 8 when (a) 2τ = 14 μs and (b) 2τ = 60 μs.

detection of the remaining signal by cross-polarization to ^{13}C and ^{29}Si measures the decay of transverse magnetization during the time 2τ of the first two pulses. The resulting T_{2H} data are in Table 7. When protons in different environments of a sample, such as the Q^2, Q^3, and Q^4 sites of the parent silica, have different T_{2H} values, different fractions of residual ^{1}H transverse magnetization remain at different sites after the time 2τ. During the delay time τ_1, spin diffusion transfers net magnetization from the sites with greater to the sites with lesser residual magnetization. Figure 9 shows the results of using a short transverse relaxation time 2τ = 14 μs for the two initial pulses vs using a longer 2τ = 60 μs. The data, presented as peak height when τ_1 > 0 divided by peak height when τ_1 = 0 vs τ_c, show spin diffusion from the Q^2 sites to the Q^4 sites (Figure 9b), even though the number of Q^2 spins is much smaller than the number of Q^4 spins. Little change occurs in the relative intensity of the Q^3 signal because it both gains magnetization from Q^2 and loses magnetization to Q^4 during τ_1. In contrast, when too little time 2τ is allowed for transverse relaxation, no such variation of relative peak heights with spin diffusion time τ_1 occurs (Figure 9a). Unfortunately, this method to demonstrate spin diffusion cannot be used on the TPM–

silica and composite samples because the T_{2H} values of the protons that cross-polarize to different ^{13}C and ^{29}Si nuclei are too nearly alike.

FTIR Spectra. Changes in the OH contents of the samples on conversion of parent silica to TPM–silica to composite were detected by diffuse reflectance IR (DRIFT) spectra. The spectrum of the parent silica has a peak at 3743 cm^{-1} assigned to isolated SiOH groups, a broad hydrogen-bonded OH stretching band over 3700–2700 cm^{-1} due to both water and SiOH groups, and a peak at 1625 cm^{-1} due to water. In the spectrum of the TPM–silica, the 3743 cm^{-1} peak was absent, the hydrogen-bonded OH band was weaker and narrower, and the 1625 cm^{-1} peak was weaker but still present. Since a C=C peak of methacrylate groups also appears at 1625 cm^{-1}, there is definitely much less and maybe no water remaining in the TPM–silica. The 1625 cm^{-1} peak was absent from the spectrum of the composite, indicating that it retained no water and that methacrylate double bonds were fully polymerized. Since ^{13}C NMR carbonyl and alkene carbon peak areas indicated 15% unpolymerized methacrylate groups, we conclude that no more than 15%, and maybe none, of the methacrylate groups in the composite failed to polymerize.

Discussion

From elemental analyses, IR spectra, and MAS NMR spectra, we have gained quantitative analyses of the structures and a qualitative understanding of the dynamics of the parent colloidal silica, the TPM–silica, and the composite.

Hydrolysis of the tetraethyl orthosilicate to produce the colloidal silica particles is incomplete, as shown by residual OC_2H_5 signals in the ^{13}C CP/MAS NMR spectrum and by the carbon content from elemental analysis. The parent silica contains about 11 OH groups for every OC_2H_5 group on the Q^2 and Q^3 silicon atoms. According to previous analyses of DRIFT spectra[48] and ^1H CRAMPS (combined rotation and multiple pulse spectroscopy) NMR spectra of silica gels,[24,25] there are three types of detectable OH protons: isolated OH groups that show a stretching vibration at 3743 cm^{-1} in the IR and a broad signal centered at 1.8 ppm in the ^1H NMR that has strong heteronuclear (^1H–^{29}Si) but weak homonuclear dipolar interactions, hydrogen-bonded Si–OH groups that show a broader OH stretching band at 3700–3000 cm^{-1} in the IR and a broad ^1H NMR band at 1–8 ppm that has strong heteronuclear and homonuclear dipolar interactions, and physisorbed H_2O that shows OH stretching at 3700–2700 cm^{-1} and a ^1H NMR signal at 3.5 ppm that has only weak dipolar interactions. The SP ^{29}Si MAS NMR spectra compared with the CP spectra of our parent silica show that only 22% of the Q^4 silicon atoms have strong enough ^1H–^{29}Si dipolar interactions to cross-polarize during a limited contact time. We presume that the Q^4 silicon atoms that do cross-polarize have at least one Q^2 or Q^3 nearest neighbor and that the remaining Q^4 silicon atoms, which are more distant from protons, have only other Q^4 nearest neighbors.

In all three samples spin diffusion equilibrates magnetization of all protons in much less than 0.5 s (T_{1H}). In the TPM–silica and in the composite, spin diffusion is almost complete in the time of $T_{1\rho H}$ (4–6 ms for TPM–silica and 9–13 ms for the composite). However, in the parent silica, which contains fewer protons, the significantly different values of $T_{1\rho H}$ of the parent silica detected via ^{13}C vs ^{29}Si proves that many of the protons dipolar coupled to the ^{29}Si nuclei are different from those dipolar coupled to ^{13}C nuclei, for otherwise all peaks in the spectrum would have the same $T_{1\rho H}$. Thus much of the cross-polarization of ^{29}Si nuclei must come from OH, not OC_2H_5 groups. Derivatization of the silica surface with TPM removes the isolated OH groups according to elemental analysis and to the disappearance of the IR band at 3743 cm^{-1}. The much shorter $T_{1\rho H}$ values of TPM-silica detected via the T^2 and T^3 sites than of parent silica detected via the Q^3 and Q^4 sites also suggest that OH groups dipolar coupled to ^{29}Si disappear during the surface derivatization.

The longer $T_{1\rho H}$ values of the composite than of the TPM–silica are due to less efficient relaxation of the protons by molecular motions at the 42–50 kHz frequencies of the proton B_1 fields in the PMMA of the composite than in the TPM layer of the TPM–silica.

Time constants $T_{1\rho C}$ for carbon relaxation in the rotating frame could depend on spin dynamics, motional dynamics, or both.[49–51] The relative contributions can be analyzed quantitatively from measured values of both $T_{1\rho C}$ and T_{IS}(ADRF) (adiabatic demagnetization in the rotating frame), the time constant for cross-polarization from protons in the local dipolar field to carbons in the applied field.[49] Analysis of a wide variety of materials indicates that spin dynamics control $T_{1\rho C}$ at 37 kHz for highly crystalline materials such as glycine, high-density polyethylene, and poly(oxymethylene) and that mainly motional contributions control $T_{1\rho C}$ in noncrystalline polymers such as polystyrenes, Bisphenol-A polycarbonate, poly(ethylene terephthalate), and PMMA.[51] We have not measured T_{IS}(ADRF), but analogy to these known polymers strongly suggests that $T_{1\rho C}$ of our parent silica and TPM–silica also depends mainly on molecular motion.

The relaxation rate $(T_{1\rho C})^{-1}$ depends on contributions from the local magnetic dipolar fields B_{loc} from neighboring protons, the precession frequency ω_1 in the spin-lock field, and the rotational correlation time τ_c according to eq 1.

$$(T_{1\rho C})^{-1} = B_{loc}^2\tau_c/(1 + \omega_1^2\tau_c^2) \qquad (1)$$

The carbon spin-lock strength in all experiments here is $\omega_1/2\pi = 50$ kHz. For ^{13}C nuclei having directly bound protons, the B_{loc} and τ_c both depend on molecular motion. If the variations in B_{loc} can be neglected, the shortest $T_{1\rho C}$ will occur when motional frequencies match the precession frequency ω_1. The data in Table 5 indicate that molecular motions most nearly match the experimental spin-lock frequency in the TPM–silica sample, in which four structurally different CH_2 groups all have $T_{1\rho C}$ of about 7 ms. The $T_{1\rho C}$ values of the unprotonated and methyl ^{13}C nuclei are longer because greater distance from protons and rapid rotation about single bonds, respectively, result in much weaker static dipolar fields. The $T_{1\rho C}$ values of the composite and PMMA are the same within experimental error and, with the exception of the $C–CH_3$ group, which undergoes internal rotation, are longer than those of the TPM–silica. Since the PMMA is well below the glass transition temperature, and the TPM groups of the TPM silica should have some rotational freedom, any main chain and side chain motions (other than methyl group rotation) in the PMMA and the composite must be at less than the 50 kHz frequencies required for efficient relaxation.

The ^1H–^1H dipolar dephasing times, T_{DH}, are about equal for the CH protons in the parent silica and in the TPM–silica, and greater for the OH protons that cross-

polarize ^{29}Si in the parent silica, which indicates weaker dipolar interaction among OH protons than among the CH protons. The lesser T_{DH} of Q^4 than of Q^2 and Q^3 in the parent silica indicates stronger dipolar interactions involving those OH groups nearest Q^4, which are probably isolated OH groups at Q^3 sites previously shown to have strong dipolar interactions in silica gel.[26] The much shorter T_{DH} values for the composite and PMMA show that PMMA is more rigid than the coupling agent on the TPM–silica surface, which is also the conclusion drawn from $T_{1\rho C}$ values.

In summary, all of the structural and relaxation NMR data lead to the following picture of the composite material. The parent silica has ethoxy groups isolated in the matrix and OH groups on the surface. The ethoxy groups in the matrix are retained during reaction with TPM, while the OH groups are consumed. The protons in the parent silica are only weakly dipolar coupled. The reaction with TPM deposits a 2 nm layer on the surface of the 10.5 nm diameter silica particles. That layer has dangling chains with considerable motion at kilohertz frequencies indicated by short $T_{1\rho C}$ and by slower ^1H–^1H dipolar dephasing than in the more rigid PMMA and composite. At least 85% of the methacrylate groups of the TPM copolymerize with MMA to cross-link the silica into the composite, which has relaxation behavior similar to that of PMMA itself.

Acknowledgment. This research was supported by National Science Foundation grants DMR9024858 for composite materials and DMR9202755 for acquisition of the NMR spectrometer. We thank Roger Assink (Sandia National Laboratory) and Corinna Czekaj (Oklahoma State University) for helpful discussions.

References and Notes

(1) Iler, R. K. *The Chemistry of Silica*; Wiley: New York, 1979; pp 582–588.
(2) Plueddemann, E. P. *Silane Coupling Agents*, 2nd ed.; Plenum: New York, 1991; pp 183–220.
(3) Mark, J. E.; Lee, C. Y.-C.; Biancone, P. A., Eds. *Hybrid Organic–Inorganic Composites*; ACS Symposium Series 585; American Chemical Society: Washington, DC, 1995.
(4) Brinker, C. J.; Scherer, G. W. *Sol–Gel Science*; Academic; New York, 1990.
(5) Sanchez, C.; Ribot, R. *New J. Chem.* **1994**, *18*, 1007.
(6) Mark, J. *J. Appl. Polym. Sci., Appl. Polym. Symp.* **1992**, *50*, 273.
(7) Sun, C.-C.; Mark, J. E. *Polymer* **1989**, *30*, 104.
(8) Fitzgerald, J. J.; Landry, C. J. T.; Pochan, J. M. *Macromolecules* **1992**, *25*, 3715.
(9) Landry, C. J. T.; Coltrain, B. K.; Brady, B. K. *Polymer* **1992**, *33*, 1486.
(10) Morikawa, A.; Yamaguchi, H.; Kakimoto, M.; Imai, Y. *Chem Mater.* **1994**, *6*, 913.
(11) Wang, W.; Ahmad, Z.; Mark, J. E. *Chem. Mater.* **1994**, *6*, 943.
(12) Pope, E. J. A.; Asami, M.; Mackenzie, J. D. *J. Mater. Res.* **1989**, *4*, 1018.
(13) Chiang, C.-H.; Liu, N.; Koenig, J. L. *J. Colloid Interface Sci.* **1981**, *86*, 26.
(14) Maciel, G. E.; Sindorf, D. W.; Bartuska, V. J. *J. Chromatogr.* **1981**, *205*, 438.
(15) Sindorf, D. W.; Maciel, G. E. *J. Am. Chem. Soc.* **1981**, *103*, 4263.
(16) Sindorf, D. W.; Maciel, G. E. *J. Am. Chem. Soc.* **1983**, *105*, 3767.
(17) Sindorf, D. W.; Maciel, G. E. *J. Phys. Chem.* **1983**, *87*, 5516.
(18) Bayer, E.; Albert, K.; Reiners, J.; Nieder, M.; Müller, D. *J. Chromatogr.* **1983**, *264*, 197.
(19) Fyfe, C. A.; Gobbi, G. C.; Kennedy, G. J. *J. Phys. Chem.* **1985**, *89*, 277.
(20) Kohler, J.; Chase, D. B.; Farlee, R. D.; Vega, A. J.; Kirkland, J. J. *J. Chromatogr.* **1986**, *352*, 275.
(21) Sudhölter, E. J. R.; Huis, R.; Hays, G. R.; Alma, N. C. M. *J. Colloid Interface Sci.* **1986**, *103*, 554.
(22) Caravajal, G. S.; Leyden, D. E.; Quinting, G. R.; Maciel, G. E. *Anal. Chem.* **1988**, *60*, 1776.
(23) Vankan, J. M. J.; Ponjee, J. J.; De Haan, J. W.; van de Ven, L. J. M. *J. Colloid Interface Sci.* **1988**, *126*, 604.
(24) Bronnimann, C. E.; Zeigler, R. C.; Maciel, G. E. *J. Am. Chem. Soc.* **1988**, *110*, 2023.
(25) Kinney, D. R.; Chuang, I.; Maciel, G. E. *J. Am. Chem. Soc.* **1993**, *115*, 6786.
(26) Chuang, I.; Kinney, D. R.; Bronnimann, C. E.; Zeigler, R. C.; Maciel, G. E. *J. Phys. Chem.* **1992**, *96*, 4027.
(27) Chuang, I.; Kinney, D. R.; Maciel, G. E. *J. Am. Chem. Soc.* **1993**, *115*, 8695.
(28) Glaser, R. H.; Wilkes, G. L.; Bronnimann, C. E. *J. Non-Cryst. Solids* **1989**, *113*, 73.
(29) Kelusky, E. C.; Fyfe, C. A. *J. Am. Chem. Soc.* **1986**, *108*, 1746.
(30) Gangoda, M.; Gilpin, R. K.; Figueirinhas, J. *J. Phys. Chem.* **1989**, *93*, 4815.
(31) Kang, H.-J.; Blum, F. D. *J. Phys. Chem.* **1991**, *95*, 9391.
(32) Gambogi, J. E.; Blum, F. D. *Macromolecules* **1992**, *25*, 4526.
(33) Weeding, T. L.; Veeman, W. S.; Jenneskens, L. W.; Gaur, H. A.; Schuurs, H. E. C.; Huysmans, W. G. B. *Macromolecules* **1989**, *22*, 706.
(34) Huijgen, T. P.; Gaur, H. A.; Weeding, T. L.; Jenneskens, L. W.; Schuurs, H. E. C.; Huysmans, W. G. B.; Veeman, W. S. *Macromolecules* **1990**, *23*, 3063.
(35) Hoh, K.; Ishida, H.; Koenig, J. L. *Polym. Compos.* **1990**, *11*, 121.
(36) Zumbulyadis, N.; O'Reilly, J. M. *Macromolecules* **1991**, *24*, 5294.
(37) Sunkara, H. B.; Jethmalani, J. M.; Ford, W. T. *Chem. Mater.* **1994**, *6*, 362.
(38) Sunkara, H. B.; Jethmalani, J. M.; Ford, W. T. *ACS Symp. Ser.* **1995**, *585*, 181.
(39) Stöber, W.; Fink, A.; Bohn, E. *J. Colloid Interface Sci.* **1968**, *26*, 62.
(40) Philipse, A. P.; Vrij, A. *J. Colloid Interface Sci.* **1989**, *128*, 121.
(41) Badley, R. D.; Ford, W. T.; McEnroe, F. J.; Assink, R. A. *Langmuir* **1990**, *6*, 792.
(42) Badley, R. D.; Ford, W. T.; McEnroe, F. J.; Assink, R. A. In *Chemically Modified Oxide Surfaces*; Leyden, D. E, Collins, W. T., Eds.; Gordon and Breach: New York, 1990; pp 295–303.
(43) van Blaaderen, A.; Vrij, A. *Adv. Chem. Ser.* **1994**, *234*, 83.
(44) Bogush, G. H.; Tracy, M. A.; Zukoski, C. F. *J. Non-Cryst. Solids* **1988**, *104*, 95.
(45) Zhang, S.; Czekaj, C. L.; Ford, W. T. *J. Magn. Reson., Ser. A* **1994**, *111*, 87.
(46) Fyfe, C. A.; Niu, J. *Macromolecules* **1995**, *28*, 3894.
(47) Rhim, W. K.; Pines, A.; Waugh, J. S. *Phys. Rev. B* **1971**, *3*, 684.
(48) Hair, M. L. In *Chemically Modified Surfaces, Silane Surfaces and Interfaces*; Leyden, D. E., Ed.; Gordon and Breach: New York, 1986; Vol. 1, pp 25–41.
(49) Steger, T. R.; Schaefer, J.; Stejskal, E. O.; McKay, R. A. *Macromolecules* **1980**, *13*, 1127.
(50) Sefcik, M. D.; Schaefer, J.; Stejskal, E. O.; McKay, R. A. *Macromolecules* **1980**, *13*, 1132.
(51) Schaefer, J.; Sefcik, M. D.; Stejskal, E. O.; McKay, R. A. *Macromolecules* **1984**, *17*, 1118.

MA951111Z